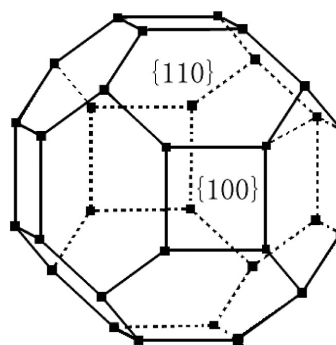
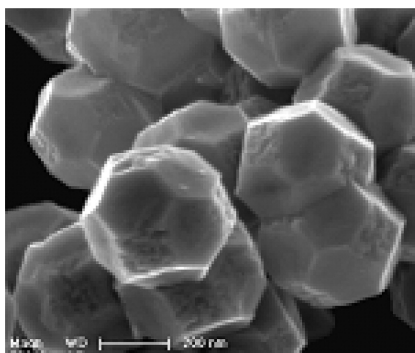


## High Symmetric 18-Facet Polyhedron Nanocrystals of CuS with a Hollow Nanocage

Hongliang Cao, Xuefeng Qian, Cheng Wang, Xiaodong Ma, Jie Yin, and Zikang Zhu

*J. Am. Chem. Soc.*, **2005**, 127 (46), 16024-16025 • DOI: 10.1021/ja055265y • Publication Date (Web): 28 October 2005

Downloaded from <http://pubs.acs.org> on March 25, 2009



### More About This Article

Additional resources and features associated with this article are available within the HTML version:

- Supporting Information
- Links to the 21 articles that cite this article, as of the time of this article download
- Access to high resolution figures
- Links to articles and content related to this article
- Copyright permission to reproduce figures and/or text from this article

[View the Full Text HTML](#)



## High Symmetric 18-Facet Polyhedron Nanocrystals of $\text{Cu}_7\text{S}_4$ with a Hollow Nanocage

Hongliang Cao,<sup>†</sup> Xuefeng Qian,<sup>\*,†</sup> Cheng Wang,<sup>\*,‡</sup> Xiaodong Ma,<sup>†</sup> Jie Yin,<sup>†</sup> and Zikang Zhu<sup>†</sup>

School of Chemistry and Chemical Technology, Shanghai Jiao Tong University, Shanghai 200240, P. R. China, and Key Laboratory of Rare Earth Chemistry and Physics, Changchun Institute of Applied Chemistry, Chinese Academy of Sciences, Changchun 130022, P. R. China

Received August 3, 2005; E-mail: xfqian@sjtu.edu.cn; cwang@ciac.jl.cn

The development of nano- or micromaterials with size- and shape-controlled morphologies may open new opportunities in exploring material chemical and physical properties.<sup>1</sup> Hollow structures have attracted great attention due to their widespread potential applications in catalysis, drug delivery, lightweight filler, acoustic insulation, photonic crystals,<sup>2</sup> and so on. However, in most cases, only spherical hollow structures have been synthesized through the use of removable templates or droplets.<sup>3</sup> Recently, some anisotropic hollow inorganic nanostructures with regular morphologies have been prepared through different synthetic strategies. Examples include octahedral  $\text{SnO}_2$ <sup>4</sup> and hexagon-based drums of  $\text{ZnO}$ ,<sup>5</sup> etc. Herein we report the synthesis of high symmetric 18-facet polyhedron of nanocrystalline  $\text{Cu}_7\text{S}_4$  with regular hollow structure based on the Kirkendall Effect<sup>6</sup> and converted it from cubic cuprous oxide nanocrystals. Copper sulfide and oxide are chosen in this work due to their potential applications in solar energy conversion, fast-ion and electrical conduction, and catalytic reaction as well.<sup>7</sup>

As one of the nonstoichiometric copper sulfides,  $\text{Cu}_7\text{S}_4$  with a Cu/S ratio of 1.75 is known as anilite and was discovered as a new low-temperature mineral phase in 1969 by Morimoto et al.<sup>8</sup> Synthetic approaches to anilite could be fulfilled by reaction of an aqueous suspension of  $\text{Cu}_2\text{O}$  with  $\text{H}_2\text{S}$ <sup>9</sup> or sulfuring agent with a solution of a metal salt.<sup>10</sup> Our synthetic strategy resembles the former one and involves following processes. First, cubic  $\text{Cu}_2\text{O}$  nanoparticles were prepared by adding weak reductive agent (ascorbic acid solution) into  $\text{Cu}^{2+}$  aqueous solution with the use of PVP (poly(vinylpyrrolidone)) as capping agents, then hollow  $\text{Cu}_7\text{S}_4$  nanocages were obtained by adding a sulfur source (thiourea) under heating conditions. Details of the experiments are provided in Supporting Information.

Before addition of thiourea, cubic cuprous oxide, which mirrors its crystal nature, could be formed under experimental conditions. The mechanism for this process has been well documented in the literature.<sup>11</sup> Pure cubic phase of  $\text{Cu}_2\text{O}$ , as shown in Figure s1A (JCPDS card No. 05-0667) and Figure s2 in Supporting Information, could be obtained in our system. After addition of thiourea into the reaction mixture and increasing the temperature to 90 °C, a gradual conversion of  $\text{Cu}_2\text{O}$  to  $\text{Cu}_7\text{S}_4$  could be observed as shown in Figure s1B (Supporting Information), where patterns of both cubic  $\text{Cu}_2\text{O}$  and monoclinic  $\text{Cu}_7\text{S}_4$  (JCPDS No. 23-958) could be indexed for products obtained by heating the reaction system for 3 h. The conversion could be completed (Figure s1C) by prolonging the reaction time to 6 h or longer. On the basis of the amount of added copper ions, the yield of  $\text{Cu}_7\text{S}_4$  is larger than 95%.

From SEM results (Figure 1A and 1B), we can find that uniform high symmetric 18-face polyhedron nanocrystals with particle size

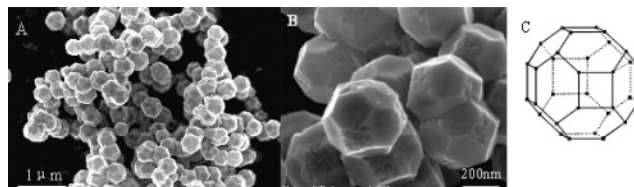


**Figure 1.** Typical FESEM images of as-synthesized 18-facet  $\text{Cu}_7\text{S}_4$  nanocrystal and its simulated structure: (A) low magnification, (B) high magnification, and (C) simulated structure.

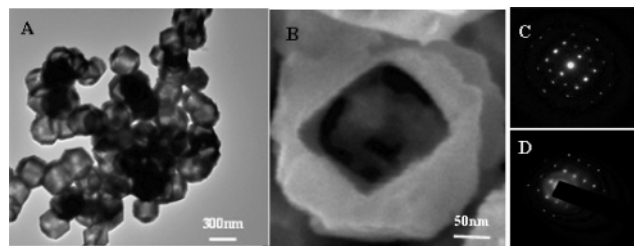


**Figure 2.** (A) TEM of polyhedral  $\text{Cu}_7\text{S}_4$  nanocrystals; (B) FESEM of broken polyhedral  $\text{Cu}_7\text{S}_4$  with regular shape void; (C) and (D) SAED of two polyhedra with their square and hexagon facets oriented perpendicular to the electron beam.

of around 320 nm are almost the exclusive products in our synthesis. In this polyhedron, it contains 18 facets, 32 vertices, and 48 edges, as shown in the simulated structure (Figure 1C). As a simple connected polyhedron, it follows the Euler's Formula,<sup>12</sup> which related the number of polyhedron vertices  $V$ , faces  $F$ , and edges  $E$  as

$$V + F - E = 2$$

There are two types of faces in this structure: six square and twelve hexagon planes. Therefore, it is not Platonic polyhedron (one type of face). For the vertices, there are also two types. One is the joint of three hexagons, and the other one is the joint of two hexagons and one square. So this polyhedron is not Archimedean polyhedron (vertices are identical) either. Among the 48 edges, 24 edges with larger length form 6 square faces, and the rest of the 24 are shorter in length and form eight vertices, which are the joints of each of the three neighboring hexagons. This structure can also be viewed as a result of cutting the 12 edges of a cube. It bears all the symmetric elements that a cube has and belongs to  $O_h$  point group.

TEM result of the 18-facet  $\text{Cu}_7\text{S}_4$  nanocrystals is shown in Figure 2A. The particles look octahedral or hexagonal in shape under TEM depending on whether the particles are sitting on an even number (4 and 2) fold axis (corresponding to octahedral shape) or a 3-fold axis (corresponding to hexagonal shape). Another important phenomenon observed here is the obvious difference in terms of

<sup>†</sup> Shanghai Jiao Tong University.

<sup>‡</sup> Changchun Institute of Applied Chemistry.

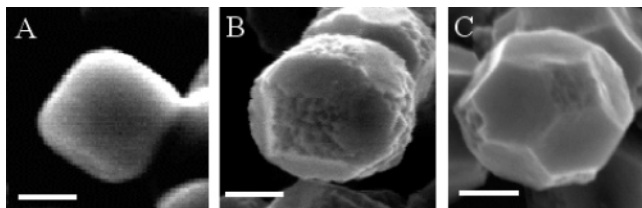


**Figure 3.** FESEM images of products at different stages: (A) pure truncated cubic  $\text{Cu}_2\text{O}$ ; (B)  $\text{Cu}_2\text{O}$  and copper sulfides nanocomposite at reaction time of 3 h; (C)  $\text{Cu}_7\text{S}_4$  polyhedron at reaction time of 6 h. Scale bar: 100 nm.

contrast between the central and fringe part of each individual particle. The darker fringe appearance implies that the nanoparticles may have a void inside. To prove this, we sonicated the samples for 2 h in order to break particles into pieces before taking the SEM image. The result in Figure 2B does show the existence of a regular-shaped void within the nanocrystals. The select area electron diffractions (SAED), recorded on the two sets of the  $\text{Cu}_7\text{S}_4$  polyhedron face, show that both faces are well crystallized.

The formation of nanocages within the particles is believed to be the result of Kirkendall Effect, which was first introduced to nanomaterial synthesis by Sun and Xia<sup>6a</sup> and was well explained by Yin et al.<sup>6b</sup> In our process, truncated nanocubic  $\text{Cu}_2\text{O}$  was formed first. When thiourea was added and subjected to heat treatment, sulfur ions were released from thiourea upon a hydrolyzation process. On the surface of nanocubic  $\text{Cu}_2\text{O}$ , a thin layer of  $\text{Cu}_7\text{S}_4$  was formed. This thin layer acts as an interface and separates the inner copper ions or  $\text{Cu}_2\text{O}$  from the outside sulfur ions. Therefore, a direct chemical reaction is hindered, and further reaction depends on the diffusion of copper or sulfur ions through this interface. The interface consists of a sulfide shell with lots of vacancies, and part of the vacancies are filled with copper ions. This specific structure allows the diffusion of copper ions from the inner part to the surface of nanoparticles and makes the conversion to  $\text{Cu}_7\text{S}_4$  feasible, provided that there are plenty of sulfur ions in the bulk solution and other experimental conditions are satisfied. Due to the big size of sulfur ions, the diffusion of sulfur ions through the interface is negligible. The formation of voids within the particle is due to gradual outward movement of copper ions; as a result, particles tend to grow in size during the conversion courses. The Kirkendall Effect process for the formation of  $\text{Cu}_7\text{S}_4$  is depicted in Figure S3 of Supporting Information, where we use a SEM picture of one intermediate particle to describe this conversion. In Figure 3, we show FESEM pictures of products obtained at different synthetic stages to support this mechanism.

According to Gibbs–Wulff's<sup>13</sup> theorem

$$\frac{\gamma_1}{h_1} = \frac{\gamma_2}{h_2} = \frac{\gamma_3}{h_3} = \dots = \text{constant}$$

where  $\gamma_n$  is the surface tension of crystal face  $n$ , and  $h_n$  is the distance of that face from the Wulff's point in the crystal. Higher surface tension faces tend to grow along its normal direction and eventually disappear from the final appearance. For cubic phase, a sequence of  $\gamma_{\{111\}} < \gamma_{\{100\}} < \gamma_{\{110\}}$  can be easily deduced from the distances between these three faces and the central Wulff's point.<sup>13,14</sup> However, if the size of the nanocrystals is smaller than 15 nm, some higher energy surfaces may still be retained due to the incomplete evolution, and spherical morphology is usually observed. Another variation from Wulff's theorem is using additives to tune the surface energies of specific crystallographic faces. For the 18-facet  $\text{Cu}_7\text{S}_4$  obtained here, the two surfaces can be assigned as  $\{110\}$  for hexagon and  $\{100\}$  for square, respectively. With the

presence of organic additives, which tend to be absorbed by  $\{110\}$ , the  $\gamma_{\{110\}}$  becomes the lowest among the three kinds of faces  $\{111\}$ ,  $\{100\}$ , and  $\{110\}$  (if  $\gamma_{\{111\}}$  is the lowest among them, it would form 14-facet nanocrystal according to ref 14). We also noticed that the square surfaces on the nanocrystals are rougher than hexagonal faces under SEM (Figure 3B and C). This could serve as a direct evidence that  $\gamma_{\{100\}}$  is larger than  $\gamma_{\{110\}}$ , as we know higher surface energy can lead to a rougher surface during the growth process. The growth along the direction normal to the  $\{100\}$  faces makes the  $\{110\}$  prominent in the final morphology and leads to the formation of 18-facet nanocrystals.

In summary, high symmetric 18-facet nanocrystals of  $\text{Cu}_7\text{S}_4$  could be formed in an aqueous approach. When converted from  $\text{Cu}_2\text{O}$  to  $\text{Cu}_7\text{S}_4$ , the crystal structure changes from cubic to monoclinic. Although the cubic morphology of  $\text{Cu}_2\text{O}$  was not retained by  $\text{Cu}_7\text{S}_4$  during the conversion, the formation of 18-facet polyhedral  $\text{Cu}_7\text{S}_4$  is still based on the growth of the cubic skeleton. At present, we are not clear why the monoclinic crystal structure of  $\text{Cu}_7\text{S}_4$  does not have significant effects on its final morphology. We believe this might be another induction that makes  $\gamma_{\{110\}}$  smaller than  $\gamma_{\{111\}}$  and  $\gamma_{\{100\}}$ . Further investigations are underway in order to uncover the underlined principles for this observation. We are also trying to use other organic additives to study their influence on the morphology variations during the conversion process based on Kirkendall Effect.

**Acknowledgment.** This work is supported by the National Natural Foundation of China (50103006), the Shanghai Shu Guang Project, the Shanghai Nano-Project. C.W. is grateful for the support from Changchun Institute of Applied Chemistry.

**Supporting Information Available:** Details of experiments and XRD patterns, and evolution schemes of 18-facet  $\text{Cu}_7\text{S}_4$  nanocrystals obtained at different synthetic stage. FESEM and TEM pictures of pure cubic  $\text{Cu}_2\text{O}$  nanocrystals. This material is available free of charge via the Internet at <http://pubs.acs.org>.

## References

- (1) MacLachlan, M. J.; Manners, I.; Ozin, G. A. *Adv. Mater.* **2000**, *12*, 675.
- (2) Caruso, F. *Chem.—Eur. J.* **2000**, *6*, 413.
- (3) (a) Liang, Z. J.; Susha, A.; Caruso, F. *Chem. Mater.* **2003**, *15*, 3176. (b) Wang, L.; Sasaki, T.; Ebina, Y.; Kurashima, K.; Watanabe, M. *Chem. Mater.* **2002**, *14*, 4827. (c) Kanungo, M.; Deepa, P. N.; Collinson, M. M. *Chem. Mater.* **2004**, *16*, 5535. (d) Dhas, N. A.; Suslick, K. S. *J. Am. Chem. Soc.* **2005**, *127*, 2368. (e) Schmidt, H. T.; Gray, B. L.; Wingert, P. A.; Ostafin, A. E. *Chem. Mater.* **2004**, *16*, 4942. (f) Fujiwara, M.; Shiokawa, K.; Tannaka, Y.; Nakahara, Y. *Chem. Mater.* **2004**, *16*, 5420.
- (4) Yang, H. G.; Zeng, H. C. *Angew. Chem., Int. Ed.* **2004**, *43*, 5930.
- (5) (a) Gao, P. X.; Wang, Z. L. *J. Am. Chem. Soc.* **2003**, *125*, 11299. (b) Jiang, Z. Y.; Xie, Z. X.; Zhang, X. H.; Lin, S. C.; Xu, T.; Xie, S. Y.; Huang, R. B.; Zheng, L. S. *Adv. Mater.* **2004**, *16*, 904.
- (6) (a) Sun, Y. G.; Xia, Y. N. *Science* **2002**, *298*, 2176. (b) Yin, Y. D.; Rioux, R. M.; Erdonmez, C. K.; Hughes, S.; Somorjai, G. A.; Alivisatos, A. P. *Science* **2004**, *304*, 711. (c) Yang, Y. J.; Qi, L. M.; Lu, C. H.; Ma, J. M.; Cheng, H. M. *Angew. Chem., Int. Ed.* **2005**, *44*, 598. (d) Wang, Y. L.; Cai, L.; Xia, Y. N. *Adv. Mater.* **2005**, *17*, 473. (e) Liu, B.; Zeng, H. C. *J. Am. Chem. Soc.* **2004**, *126*, 16744.
- (7) (a) Nair, M. T. S.; Nair, P. K. *Semicond. Sci. Technol.* **1989**, *4*, 191. (b) Pala, N.; Rumyantsev, S. L.; Sinius, J.; Talapatra, S.; Shur, M. S.; Gaska, R. *Electron. Lett.* **2004**, *40*, 273. (c) Hara, M.; Kondo, T.; Komoda, M.; Ikeda, S.; Shinohara, K.; Tanaka, A.; Kondo, J.; Domen, K. *Chem. Commun.* **1998**, 357. (d) Musa, A. O.; Akomolafe, T.; Carter, M. J. *Sol. Energy Mater. Sol. Cells* **1998**, *51*, 305.
- (8) Morimoto, N.; Koto, K.; Shimazaki, Y. *Am. Mineral.* **1969**, *54*, 1256.
- (9) Cavallotti, P.; Salvago, G. *Electrochim. Metal.* **1969**, *4*, 181.
- (10) Vitalijus, J.; Raimondas, M.; Remigijus, I.; Ingrida A. *Colloid Polym. Sci.* **2003**, *281*, 84.
- (11) (a) Gou, L. F.; Murphy, C. J. *J. Mater. Chem.* **2004**, *14*, 735. (b) Gou, L. F.; Murphy, C. J. *Nano Lett.* **2002**, *2*, 231. (c) Chang, Y.; Zeng, H. C. *Cry. Growth Des.* **2004**, *4*, 273.
- (12) Coxeter, H. S. M. *Regular Polytopes*; New York: Dover, 1973; pp 9–11 and 165–172.
- (13) Wulff, G.; Zeitschrift, F. *Krystallogr.* **1901**, *34*, 449.
- (14) Wang, Z. L. *J. Phys. Chem. B* **2000**, *104*, 1153.

JA055265Y